Nonadiabatic effects of atomic motion inside a high-*Q* optical cavity

P. Zhang,[1] Y. Li,[1,2] C. P. Sun,[1] and L. You[1,2,3]
[1]*Institute of Theoretical Physics, The Chinese Academy of Sciences, Beijing 100080, China*
[2]*Interdisciplinary Center of Theoretical Studies, The Chinese Academy of Sciences, Beijing 100080, China*
[3]*School of Physics, Georgia Institute of Technology, Atlanta, Georgia 30332, USA*
(Received 26 November 2003; published 8 December 2004)

We revisit the topic of atomic center of mass motion of a three level atom Raman coupled strongly to an external laser field and the quantum field of a high-*Q* optical cavity. We focus on the motion related nonadiabatic effects of the atomic internal dynamics and provide a quantitative answer to the validity regime for the application of the motional insensitive dark state as recently suggested by Duan, Kuzmich, and Kimble [Phys. Rev. A **67**, 032305 (2003)].

DOI: 10.1103/PhysRevA.70.063804 PACS number(s): 42.50.Ct, 03.67.Lx, 89.70.+c, 32.80.−t

I. INTRODUCTION

The development of quantum information science and technology carries the potential of revolutionary impact on many aspects of our society, as evidenced already by the applications in quantum cryptography, quantum communication, and rudimentary quantum computing. Among the physical systems being investigated, high-*Q* optical cavities coupled with trapped atomic qubits represent a paradigm for this burgeoning field. In addition to their demonstrated abilities for controlled (and coherent) quantum dynamics of both atomic and/or cavity photonic qubits, cavity quantum electron diffraction (QED) systems are unique because they represent a prototype enabling technology for the coherent interconversion of quantum information encoded in material qubits or flying photonic qubits for propagation to far away places.

Despite much effort and spectacular advances from several groups in recent years [1–3], high fidelity deterministic logic operations even at the level of two qubits remain elusive in cavity QED based systems. Among the factors as commonly attributed to being significant road blocks, the localization of atomic motional wave packet is perhaps the most demanding. In nearly all quantum computing protocols of atoms coupled to a high-*Q* cavity field, it is essential to reach the so-called strong coupling limit, where the coherent coupling of an atom with the near resonant cavity mode g must be much larger than both the cavity decay rate κ (one side) and the atomic spontaneous emission rate γ, i.e., $g \gg \kappa$ and $g \gg \gamma$. Since g^2 is inversely proportional to the mode volume of the cavity, it typically points to small cavities in the Fabry-Perot arrangement, where the cavity mode is that of a standing wave given by

$$g(\vec{r}) = g_0 \chi(\vec{r}),$$

$$\chi(\vec{r}) = \frac{w_0}{w(z)} \exp\left[- \frac{\rho^2}{w^2(z)} \right] \sin(kz), \tag{1}$$

with $\rho = \sqrt{x^2+y^2}$ the transverse (polar) coordinate measured from the cylindrically symmetric cavity axis along the z direction. The typical geometries have the mode waist $w(z) = w_0\sqrt{1+z^2/z_0^2}$ much larger than the cavity wavelength λ, where $z_0 = \pi w_0^2/\lambda$ is the Rayleigh range. Unless each individual atomic motion is localized to much less than the resonant wavelength λ, i.e., in the so-called Lamb-Dicke limit (LDL), this position dependent uncertainty of coupling strength $g(\vec{r})$ generally spoils the quantum coherence, and prevents high fidelity quantum logic operations. This challenging limit is not so-far under complete experimental control, it is especially problematic for optical cavity QED systems.

Recently, two independent groups [4,5] have noticed an interesting scenario where the above undesirable position dependence of $g(\vec{r})$ can be largely overcome with the use of a so-called dark state, when the classical Raman laser field is assumed to have the same spatial dependence as the quantum field $g(\vec{r})$. For a large class of quantum computing protocols based on atomic cavity QED, the building block consists of a three level Λ-type atom of stable ground states $|g_0\rangle$ and $|g_1\rangle$ that couple to an excited state $|e\rangle$. Such an arrangement allows for a coherent mapping of an atomic qubit $(\alpha|g_0\rangle + \beta|g_1\rangle)$ into the photonic coherence of the cavity. In the most publicized version as originally suggested [6], it is assumed that a classical laser field and the quantum cavity field establishes a two-photon matched Raman resonance between $|g_1\rangle \leftrightarrow |e\rangle$ and $|g_0\rangle \leftrightarrow |e\rangle$. By denoting the Rabi frequency of the classical laser field as Ω, the dipole coupling in the interaction picture can be summarized as

$$H_0 = -\hbar\Delta|e\rangle\langle e| + \hbar\Omega|e\rangle\langle g_1| + \hbar g|e\rangle\langle g_0|c + \text{H.c.}, \tag{2}$$

where c is the annihilation operator for the near resonant cavity photon mode used for Raman coupling (Fig. 1), and the common detuning $\Delta = \omega_L - \omega_{eg_1} = \omega - \omega_{eg_0}$. Both atomic and cavity decays (γ or κ) are omitted in this study allowing us to concentrate on the investigation of nonadiabatic effects due to atomic motion within the coherent atom-cavity dynamics. Thus generally speaking, our model requires the total operation time to be much less than $1/\gamma$ or $1/\kappa$. It is easy to check that the following "dark state"

$$|D\rangle = \frac{1}{\sqrt{|g|^2 + |\Omega|^2}} (g|g_1,0\rangle - \Omega|g_0,1\rangle), \tag{3}$$

is an eigenstate of the Hamiltonian Eq. (2) with a zero eigenvalue, where $|0\rangle_C$ and $|1\rangle_C$ denote the Fock state of 0 or 1

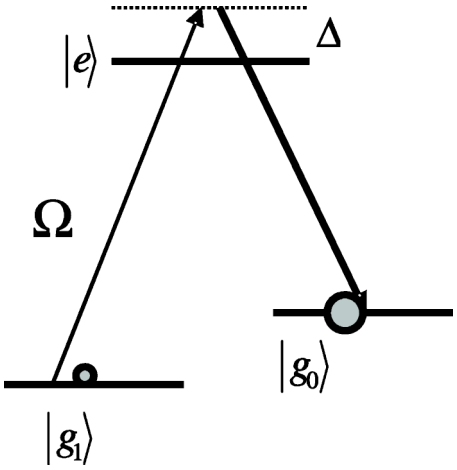

FIG. 1. Illustration of the Raman coupling.

cavity photons, respectively. It is dark, or, immune to atomic spontaneous emission because it contains no atomic excited state. By engineering a counterintuitive pulse sequence as in the STIRAP (stimulated Raman adiabatic passage), and assume the atom + cavity system to adiabatically follow the above dark state, it leads to a highly efficient protocol for converting the atomic qubit state into a photonic superposition according to [6–8]

$$(\alpha|g_0\rangle + \beta|g_1\rangle) \otimes |0\rangle_C \rightarrow |g_1\rangle \otimes (\alpha|0\rangle + \beta|1\rangle)_C. \quad (4)$$

When atomic motion is considered, the position dependence of $g(\vec{r})$ generally leads to a loss of coherence due to the potential entanglement between the motion and the atomic internal state as well as the cavity photon state. The idea of the motional insensitive protocol [4,5], assumes a classical laser field that has the same dependence as $g(\vec{r})$. Following the notation of Duan *et al.* [5], this assumption amounts to

$$\Omega(\vec{r},t) = \Omega_0(t)\chi(\vec{r}) = r_0 g_0 \alpha(t)\chi(\vec{r}). \quad (5)$$

A simple arrangement involves choosing the pump and the cavity transitions $|g_1\rangle \leftrightarrow |e\rangle$ and $|g_0\rangle \leftrightarrow |e\rangle$ to correspond the left and right circular polarized component of the same cavity mode. A more flexible setup would involve the use of a different cavity mode such that near the cavity center, $\chi(\vec{r})$ for the two modes remain almost matched as the two modes differ very little in their respective wavelengths [9].

The aim of this paper is to study in detail nonadiabatic effects of the above motion insensitive protocol. As was also noted in Ref. [5], it clearly becomes difficult to maintain adiabaticity when the atomic Raman coupling is too weak to affect the transfer, particularly near regions of small $g(\vec{r})$ values. Furthermore, an atom remaining in the dark state essentially experiences no light force from the combined fields of both the cavity mode and the external laser. This arguably leads to an upper limit on the atomic kinetic energy; the duration T for the STIRAP is determined by atomic internal state dynamics. Thus for an atom with a velocity of v_a, during the STIRAP, it will move a distance $v_a T$ if it is to remain in the dark state. A larger v_a leads simply to a large travelling distance. Nonadiabatic effects will arise if atoms were to travel far enough to cross nodal planes of $\chi(\vec{r})$ (as we will see later this contradicts the discussion of a better satisfied adiabatic condition near nodal points as in Ref. [5]). The ideal operation of the motional insensitive protocol would require the use of trapped atoms, i.e., with atoms confined near regions of maximal $g(\vec{r})$ [5] by an external force independent of the cavity or Raman field. The trap must be strong enough to limit the atomic motion due to an amplitude smaller than half the cavity wavelength $\lambda/2$, such that nodal crossing can be completely avoided.

Another motivation for this study is the desire to understand nodal crossing dynamics in general for the Raman configuration when the trapping provided by an extra higher order cavity mode is absent as in earlier experiments [2], where either the resonant cavity field or an external laser field provided confinement of atoms (not in the dark state). Based on the dressed energy levels of an atom coupled to both fields, we find that the dynamics of an atom crossing a nodal plane can be effectively described in terms of the celebrated Landau-Zener theory [10]. Yet, a somewhat puzzling situation arises according to Landau-Zener theory which prefers to have a larger velocity v_a during the crossing in order to maintain in the initial (dark) state. Consistent with the paper of Duan *et al.* [5], the motional state insensitive protocol works only in the limit when the atoms are trapped by yet an additional mechanism such that its motion is limited to a variation of $g(\vec{r})$ within approximately a factor of 2. On the other hand, a large velocity tends to cause large amplitude motions, thus against the localization of the Lamb-Dicke limit. We thus find it interesting to study the relevant Landau-Zener transitions in order to shed light on the motional effects of atoms in cavity QED.

This paper is organized as follows. In Sec. II, we formulate the model of our study and illustrate parameter regimes of interest to current experimental efforts. Sections III and IV are devoted, respectively, to the study of the nonadiabatic level crossing in terms of a Landau-Zener transition dynamics and the comparison between numerical simulations and the approximate analytic Landau-Zener state transition formulas. We have developed an interesting analytic mapping (in the absence of an external trap) of the atomic motion through a nodal point into a Landau-Zener level crossing dynamics. Within each of the above sections, we will study various limiting cases, mainly focusing on a simple model that involves a one-dimensional motion along the cavity axis [11,12]. Finally we summarize and attempt to make some general conclusions in Sec. V. The appendixes contain several technical points that may be useful for related studies.

II. FORMULATION

In the descriptions to follow, we will assume both fields to be on resonance and take the atomic detuning $\Delta = 0$. For the more general situation as shown in Appendix A with a nonzero but constant $\Delta \neq 0$ (position independent), we find it simply leads to formally identical results as discussed here for $\Delta = 0$ (see Appendix A). When necessary, an external trap, assumed to be internal state independent is assumed to be

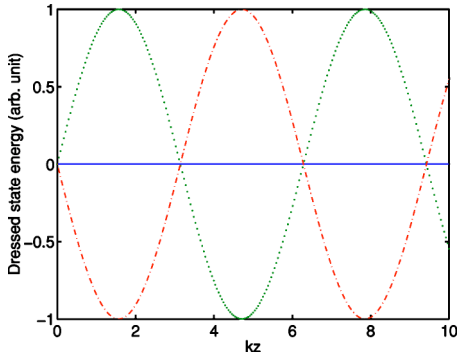

FIG. 2. Dressed energies of the coupled atom + cavity system at a particular radial location along the cavity axis z (at a fixed time t). When the atom moves through a nodal plane, nonadiabatic transfer of its internal state out of the dark state becomes a critical issue, which constitutes the main topic being studied in this work.

available and centered around the maximum of $g(\vec{r})$ to confine atomic motion to within the order of one-half the standing wave wavelength as in Ref. [5].

The Hamiltonian for atomic internal degrees of freedom (on resonance $\Delta=0$) can be written as a $3\otimes 3$ matrix [5] in the basis $\{|e,0\rangle,|g_0,1\rangle,|g_1,0\rangle\}$,

$$H=\hbar\begin{pmatrix}0 & g & \Omega\\ g^* & 0 & 0\\ \Omega^* & 0 & 0\end{pmatrix}. \tag{6}$$

Within the semiclassical approximation for the atomic motion, the center of mass motion is described by $\vec{p}^2/2M$ with M the atomic mass and $\vec{p}$ the atomic momentum. While for slow atoms, we may wish to include the associated forces due to the atomic interaction with the spatially dependent laser (cavity) fields. We will first consider the simple case of predetermined atomic motion as it corresponds to atoms staying in the dark state, i.e., we simply assume that atomic motion is not affected. We will also comparatively address the case of a trapped harmonic atom motion. We defer the inclusion of atomic dipole forces to a future investigation. With these assumptions, we find the three eigenvalues

$$E_0=0,$$

$$E_\pm=\pm\chi[r(t)]g_0\sqrt{1+|r_0\alpha(t)|^2}, \tag{7}$$

where $E_\pm$ depends on $\vec{r}$. Here, we have used $\Omega=r_0\alpha(t)g$, $|g|=|\chi[r(t)]g_0|$, and $\sqrt{|g|^2+|\Omega|^2}=|\chi[r(t)]g_0|\sqrt{1+|r_0\alpha(t)|^2}$. We note that $E_+>E_-$ when $\chi[r(t)]g_0>0$, and $E_+<E_-$ when $\chi[r(t)]g_0<0$.

Figure 2 shows the atomic dressed state energies (7) along the cavity axis at a given radial location ($\Delta=0$) for a fixed time t when the external laser is turned on. For an atom to cross a nodal plane, it must be initially within a distance reachable within the duration of the external pump pulse $\alpha(t)$ with its initial velocity.

In addition to dark state (3), the two other eigenstates are

$$|B_\pm\rangle=\frac{1}{\sqrt{2}}(|B\rangle\pm|e,0\rangle),$$

$$|B\rangle=\frac{e^{i\phi}}{\sqrt{1+|r_0\alpha(t)|^2}}[|g_0,1\rangle+r_0^*\alpha(t)|g_1,0\rangle], \tag{8}$$

where $e^{i\phi}=g^*/|g|$ and will be assumed to be unity later.

Before writing down the Schrödinger equation, we absorb the phase factors due to the adiabatic evolution along each of the above (time-dependent) eigenstates,

$$|\Psi(t)\rangle=\sum_{n=0,+,-}C_n(t)e^{-i\int_0^t E_n(t)dt'/\hbar}|n\rangle, \tag{9}$$

where we have used the shorthand notation of $n=0$ for the dark state $|D\rangle$ and $n=\pm$ for states $|B_\pm\rangle$, respectively. The coefficients C_n are governed by

$$\dot{C}_0=-e^{-i\int_0^t E_+(t')dt'/\hbar}\langle D|\dot{B}_+\rangle C_+-e^{-i\int_0^t E_-(t')dt'/\hbar}\langle D|\dot{B}_-\rangle C_-,$$

$$\dot{C}_+=-e^{+i\int_0^t E_+(t')dt'/\hbar}\langle B_+|\dot{D}\rangle C_0-e^{-i\int_0^t[E_-(t')-E_+(t')]dt'/\hbar}\langle B_+|\dot{B}_-\rangle C_-,$$

$$\dot{C}_-=-e^{i\int_0^t E_-(t')dt'/\hbar}\langle B_-|\dot{D}\rangle C_0-e^{-i\int_0^t[E_+(t')-E_-(t')]dt'/\hbar}\langle B_-|\dot{B}_+\rangle C_+. \tag{10}$$

We now assume that $\alpha(t)$ is a real parameter, which leads to

$$\langle B_\pm|\dot{B}_\mp\rangle=\frac{1}{2}\langle B|\dot{B}\rangle=0,$$

$$\langle D|\dot{B}_\pm\rangle=\frac{1}{\sqrt{2}}\langle D|\dot{B}\rangle=\frac{r_0^*\dot{\alpha}(t)}{\sqrt{2}(1+|r_0\alpha(t)|^2)}. \tag{11}$$

Denoting $E_\pm=\pm\varepsilon$, we end up with the simplified form of Eq. (10),

$$\dot{C}_0=-e^{-i\int_0^t\varepsilon(t')dt'/\hbar}K(t)C_+-e^{i\int_0^t\varepsilon(t')dt'/\hbar}K(t)C_-,$$

$$\dot{C}_+=e^{+i\int_0^t\varepsilon(t')dt'/\hbar}K^*(t)C_0,$$

$$\dot{C}_-=e^{-i\int_0^t\varepsilon(t')dt'/\hbar}K^*(t)C_0, \tag{12}$$

with

$$K(t)=\frac{r_0^*\dot{\alpha}(t)}{\sqrt{2}[1+|r_0\alpha(t)|^2]}=\langle D|\dot{B}_\pm\rangle. \tag{13}$$

These equations can be numerically integrated using standard algorithms to investigate nonadiabatic level crossings. Before attempting an analytical understanding of the level crossing dynamics near the nodes of the cavity mode function $\chi(\vec{r})$ in the next section, we first consider here typical regimes of system parameters.

A. Parameters

We will use Cs as a prototype atom for the estimation of various atomic parameters. The resonant transition between

the $6^2S_{1/2}$ and $6^2P_{3/2}$ (unclear spin $I=7/2$), occurs at around $\lambda=852.35$ (nm), $\hbar\omega=1.455$ (eV), and excited state lifetime $(1/\gamma)=30.70$ (ns), or $\gamma=(2\pi)5.18$ (MHz). The recoil frequency of resonant transition is about $\omega_R=\hbar k^2/(2M)=2.07$ (kHz), corresponding to a temperature of 0.198 (μK), or a recoil velocity of 0.352 (cm/s). The wavelength of $\lambda_{\mathrm{FORT}}=936$ (nm) used for the dipole trapping of atoms in Ref. [5] corresponds to a higher order cavity field.

The vacuum Rabi coupling between the cavity field and the atom is $g_0=(2\pi)50$ (MHz) as in the recent CalTech experiment [1]. For order of magnitude estimates, the ratio $r_0=\Omega/[g\alpha(t)]$ can be taken as unity.

According to Sec. III A of Ref. [5], we take the adiabatic parameter $\alpha(t)$ as a Gaussian function

$$\alpha(t)=\alpha_0\exp\left[-\frac{(t-T_0)^2}{t_W^2}\right], \tag{14}$$

with the total protocol for state transfer being approximated as $T=2T_0$. The amplitude α_0 is assumed to be 30 and the width t_W is assumed to be $T_0/3$. For the efficient operation of the quantum state transfer protocol utilizing the dark state adiabatic passage, the excited state atomic lifetime $\propto 1/\gamma$ essentially sets the time scale, for this reason we take $t_W\sim 1/\gamma$, or $T_0\sim 10/\gamma$.

Assuming that atoms are trapped inside a single well of the standing wave cavity field, or of the wells of the dressed energy $E_{\pm}(\vec{r})$, we can estimate the oscillation frequency inside according to

$$\begin{aligned} g_0\chi(\rho,z-\lambda/4) &= g_0\exp\left[-\frac{\rho^2}{w^2(z-\lambda/4)}\right]\sin(kz-\pi/2) \\ &= g_0\exp\left[-\frac{\rho^2}{w^2(z-\lambda/4)}\right]\left[2\sin^2\left(\frac{kz}{2}\right)-1\right] \\ &\approx g_0\exp\left[-\frac{\rho^2}{w^2(z)}\right]\left[\frac{(kz)^2}{2}-1\right], \end{aligned} \tag{15}$$

near the axis center where the well is deepest, which gives the strongest axial oscillation and radial oscillation according to

$$\frac{1}{2}M\omega_z^2z^2=\frac{1}{2}\hbar g_0k^2z^2, \tag{16}$$

$$\frac{1}{2}M\omega_\rho^2\rho^2=\hbar g_0\frac{\rho_2}{w^2(z)}, \tag{17}$$

i.e., we obtain

$$\omega_z=\sqrt{2g_0(\hbar k^2/2M)},$$

$$\omega_\rho=2\sqrt{g_0(\hbar k^2/2M)}\frac{1}{kw(z)}. \tag{18}$$

Given the additional enhancement due to $\Omega(\vec{r})$ in $E_{\pm}$, and use the estimated parameters as outlined above, we then take $\omega_z\sim(2\pi)500$ (kHz), and assume a fundamental cavity mode waist of $w(0)=30\lambda$, we end up with $\omega_\rho\sim(2\pi)2.65$ (kHz), of the same orders of magnitude as in Ref. [1] of the optical trap from a higher order cavity mode. Of course, these estimates are valid only for atomic motion near the bottom of the trap. For significantly higher atomic energies, as for instance in the recent experiment [1], where atomic kinetic energy is of the order of $(2\pi)20$ (MHz), or about one-half of the actual potential barriers at about $(2\pi)50$ (MHz), and about 40 $(\hbar\omega_z)$ and 7500 $(\hbar\omega_\rho)$, simple harmonic motion cannot be assumed.

Within the regimes of these parameters, atomic center of mass motion is well approximated by classical dynamics in a conservative potential. We can also estimate the maximal velocity of these atoms when trapped in the above single well potential,

$$\tfrac{1}{2}Mv_{zM}^2(\hbar k/M)^2=40(\hbar\omega_z)\sim\tfrac{1}{2}Mv_{\rho M}^2(\hbar k/M)^2=7500(\hbar\omega_\rho), \tag{19}$$

where we have expressed velocities in atomic recoil units. Thus we find

$$v_{zM}\sim v_{\rho M}=\sqrt{\frac{40\ (\mathrm{MHz})}{2\omega_R}}=\sqrt{10\,000}=100(v_R)\approx 35(\mathrm{cm/s}). \tag{20}$$

This leads to the assumption of atomic velocities with the following choices for numerical simulations; $v_z\approx 1$ (m/s) $\sim 0.036(\lambda\gamma)$ (10 times more kinetic energy), $v_z\approx 0.35$(m/s), and $v_z\approx 0.1$(m/s) (10 times less kinetic energy). With $T_0\sim 10/\gamma$, the respective distances that a typical atom travels during the state transfer protocols become 0.03–0.3 (μm), which is a significant fraction of $\lambda/4$, one-half the distance between the nearest nodal planes. It is important to emphasize that in this limit which corresponds to the recent experiment [1], atomic kinetic energy is much higher than its single photon recoil energy, and the atom's motional quantum state is much higher than the ground state of each trapped well. This lends strong support to our assumption of using a constant (predetermined) atomic trajectory in studying the level crossing dynamics. When an additional cavity field is used to confine atoms, optical dipole force is the reason for atoms to turn around at classical turning points.

B. Qualitative picture of the failure of adiabaticity

To maintain adiabaticity during atomic motion, the system must satisfy [13]

$$\left|\frac{\langle n(t)|\partial_t|m(t)\rangle}{E_n(t)-E_m(t)}\right|\ll 1, \tag{21}$$

for all adiabatic energy levels. The above notation applies to a general time dependent Hamiltonian $H(t)$ with eigenfunctions $|m(t)\rangle$ and eigenvalues $E_m(t)$. The time derivative of $|m(t)\rangle$ should be calculated according to

$$\partial_t|m(t)\rangle=\sum_{R_i}\frac{\partial}{\partial R_i}|m(t)\rangle\frac{dR_i}{dt}, \tag{22}$$

with R_i the ith parameter.

In the problem considered here, there are four parameters: α,x,y, and z. Similar to Ref. [5], we take the spatial mode

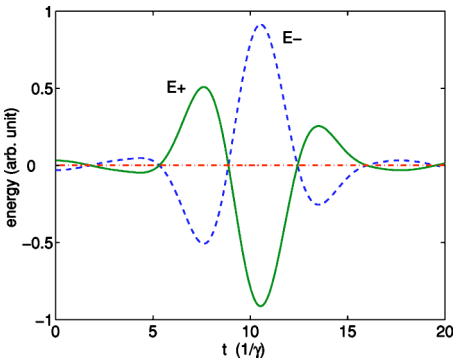

FIG. 3. The time dependent dressed state energies $E_{0/\pm}$ with the time dependent pulse shape $\alpha(t)$ as in Eq. (14). We have used $z(t)=vt$ with the speed of the atom being $v=0.14(\lambda\gamma)\approx 4(\mathrm{m/s})$. $\alpha(t)$ is assumed to begin increasing at time $t=0$ when the atom is located at the peak of the cavity field where $|\sin(kz)|=1$.

functions to be identical as in Eq. (5). It is easy to see that the dark state Eq. (3) $|D\rangle$ as well as the other two eigenstates

$$|B_{\pm}\rangle = \frac{1}{2\sqrt{g^2+\Omega^2}}(g|g_0,1\rangle + \Omega|g_1,0\rangle) \pm \frac{1}{\sqrt{2}}|e,0\rangle, \quad (23)$$

only depends on the parameter α and has nothing to do with $\vec{r}$. So the numerator of Eq. (21) is independent of the atomic speed $\vec{r}$. On the other hand, two of the three eigenvalues

$$E_{\pm} = \pm\sqrt{g^2+\Omega^2}, \quad (24)$$

do depend on $\vec{r}$. Thus the denominator of Eq. (21) depends on the position of the atom $\vec{r}$. Assuming that the time evolution of $\alpha(t)$ is uncorrelated with atomic motion $\vec{r}(t)$, the value of Eq. (21) may become large, especially in the regions where $|E_n(t)-E_m(t)| \ll |\langle n(t)|\partial_t|m(t)\rangle|$.

Two regions require special attention: (1) the nodal planes perpendicular to the cavity axis due to the standing wave term $\sin(kz)=0$; and (2) the region away from the cavity axis due to the exponentially damped Gaussian term $\exp[-\rho^2/\omega^2(z)]$. In this study, we focus on the level crossing dynamics, which happens mainly in the first region defined above. For the latest experiments, as in Refs. [1,2] where atoms are localized to a single well along the cavity axis, we may expect reduced nonadiabaticity because no actual level crossing occurs.

Before attempting a comprehensive understanding of the problem, we will first discuss the qualitative picture of how adiabatic following is violated during the atomic motion in this section. For simplicity, we will model the atomic motion as being simple one dimensional. From Eq. (13), the adiabatic condition Eq. (21) is just

$$\left|\frac{K(t)}{E_{\pm}(t)}\right| \ll 1, \quad (25)$$

where $|E_{\pm}(t)|=|\chi[r(t)]|g_0\sqrt{1+|r_0\alpha(t)|^2}$ as defined before. We see that $E_{\pm}(t)$ becomes sufficiently small (see Fig. 3) when the atom is near the nodal plane $\sin(kz)=0$, where the condition Eq. (25) is easily violated.

After elementary substitutions, we find

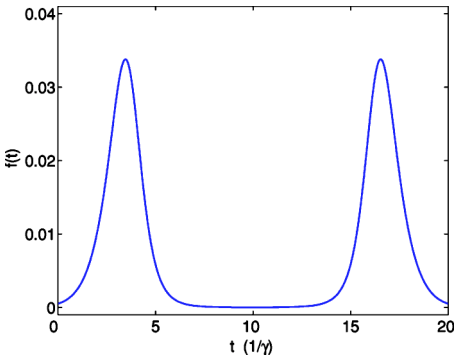

FIG. 4. The function $f(t)$ of Eq. (27).

$$\left|\frac{K(t)}{E_{\pm}(t)}\right| = \frac{f(t)}{|\sin(kz)|}, \quad (26)$$

with

$$f(t) = \left|\frac{\dot{\alpha}(t)}{\sqrt{2}g_0[1+|\alpha(t)|^2]^{3/2}}\right|. \quad (27)$$

In Fig. 4, we have graphed the function $f(t)$.

The two prominent features as in Fig. 4 at times of $3.3/\gamma$ and $16.7/\gamma$ correspond to the instants when the Gaussian shaped pulse gives rise to the largest shape changes. Apparently, $f(t)$ is significant at $t=3.3/\gamma$ and $t=16.7/\gamma$. From Eq. (26), we note if the atomic position is near a nodal plane when $|\sin(kz)|$ is small, $|K(t)/E_{\pm}(t)|$ becomes large and the adiabatic condition (25) can become severely violated at these instants. This adiabatic breakdown is less serious at $t=16.7/\gamma$ when the internal state transfer protocol is almost completed, but detrimental at $t=3.3/\gamma$, near the beginning of the process.

III. LANDAU-ZENER TRANSITIONS

As was shown from the previous discussions, the application of the adiabatic approximation can potentially fail near a nodal plane where $\chi(\vec{r})=0$. In this section, we hope to analytically investigate the transition from the dark state to bright states when the atom goes across a nodal plane.

A. One-dimensional motion along the cavity axis

We first deal with the one-dimensional case of atomic motion along the cavity axis. Assuming

$$\chi(\vec{r}) = \sin(kz), \quad (28)$$

and take the atomic motion according to $z=vt$, our problem is to solve Eq. (12), with the initial conditions

$$|C_0(-u)| = 1,$$

$$C_{\pm}(-u) = 0. \quad (29)$$

More specifically, we in fact only wish to solve for $|C_0(u)|^2$ and $|C_{\pm}(u)|^2$ after one nodal crossing.

As the lowest order approximation, we assume $\alpha(t)$ and $K(t)$ to be constants in the domain $kz\in[-u,u]$ and we also

assume that the energy $\varepsilon(t)/\hbar = \sin(kz) g_0 \sqrt{1+|\alpha(t)|^2}$ can be approximated as a linear function of time (see Appendix B) in this domain

$$\varepsilon(t)/\hbar \approx kvtg_0\sqrt{1+|\alpha(t)|^2}, \tag{30}$$

where v is a constant atomic speed along the cavity axis.

The second equation of Eq. (12) can be rewritten as

$$\begin{aligned}\frac{d^2}{dt^2}C_+ &= i\epsilon(t)\dot{C}_+/\hbar + e^{i\int_0^t \varepsilon(t')dt'/\hbar} K\dot{C}_0 \\ &= i\epsilon(t)\dot{C}_+/\hbar - e^{i\int_0^t \varepsilon(t')dt'/\hbar} K \\ &\quad \times \left(e^{-i\int_0^t \varepsilon(t')dt'/\hbar} KC_+ + e^{i\int_0^t \varepsilon(t')dt'/\hbar} KC_-\right) \\ &= i\epsilon(t)\dot{C}_+/\hbar - K^2C_+ - e^{2i\int_0^t \varepsilon(t')dt'/\hbar} K^2C_-. \end{aligned} \tag{31}$$

Using

$$\dot{C}_- = e^{-i\int_0^t \varepsilon(t')dt'/\hbar} KC_0 = e^{-2i\int_0^t \varepsilon(t')dt'/\hbar}\dot{C}_+, \tag{32}$$

and $C_\pm(-u)=0$, we find

$$\begin{aligned} C_- &= \int_{-u}^{t} e^{-2i\int_0^{t'} \varepsilon(t'')dt''/\hbar}\dot{C}_+(t')dt' = e^{-2i\int_0^{t'} \varepsilon(t'')dt''/\hbar}C_+ \\ &\quad + 2i\int_{-u}^{t} e^{-2i\int_0^{t'} \varepsilon(t'')dt''/\hbar}\varepsilon(t')C_+(t')dt'/\hbar. \end{aligned} \tag{33}$$

Substituting Eq. (33) into (31), we find

$$\begin{aligned}\frac{d^2}{dt^2}C_+ &= i\epsilon(t)\dot{C}/\hbar - 2K^2C_+ \\ &\quad + 2iK^2\int_{-u}^{t} e^{2i\int_{t'}^{t} \varepsilon(t'')dt''/\hbar}\varepsilon(t')C_+(t')dt'/\hbar. \end{aligned} \tag{34}$$

The last term is rapidly oscillating and within the lowest order approximation, it can be neglected (see Appendix C). Then the equations of C_+ and C_0 become

$$\frac{d^2}{dt^2}C_+ = i\epsilon(t)\dot{C}_+/\hbar - 2K^2C_+ \tag{35}$$

and

$$\dot{C}_+ = e^{i\int_0^t \varepsilon(t')dt'/\hbar} KC_0. \tag{36}$$

Using the transformation

$$d_0 = (-i)\frac{1}{\sqrt{2}}C_0,$$

$$c_+ = e^{-i\int_0^t \varepsilon(t')dt'/\hbar}C_+, \tag{37}$$

we find that Eq. (35) is equivalent to a problem described by an effective Hamiltonian as below

$$i\hbar\frac{\partial}{\partial t}\begin{pmatrix} d_0 \\ c_+ \end{pmatrix} = \begin{pmatrix} 0 & -\sqrt{2}\hbar K \\ -\sqrt{2}\hbar K & \varepsilon \end{pmatrix}\begin{pmatrix} d_0 \\ c_+ \end{pmatrix}, \tag{38}$$

with the initial condition

$$d_0(-u) = (-i)\frac{1}{\sqrt{2}},$$

$$c_+(-u) = 0. \tag{39}$$

Nonadiabatic effect induced transitions mainly occur within the domain $kz \in [-u,u]$, i.e., u is chosen such that beyond this domain, adiabatic condition Eq. (21) is well satisfied. In the end, as we will see later, our result is independent of the choice of u. Since $\epsilon(t)$ is a linear function of t, this problem is exactly the same one as discussed in the original Zener's paper [10]. At the edge of the domain $kz \in [-u,u]$, $|K| \ll |\epsilon|$ and the initial conditions can be adiabatically maintained to the domain $(-\infty,\infty)$, just as Zener has done. Noting the normalization condition

$$|d_0|^2 + |c_0|^2 = \tfrac{1}{2}, \tag{40}$$

and using Zener's solution [10], we find that

$$|d_0(\infty)|^2 = \frac{1}{2}\exp\left(-2\pi\frac{2K^2}{|kvg_0\sqrt{1+|\alpha|^2}|}\right), \tag{41}$$

which leads to

$$|C_+(\infty)|^2 = \frac{1}{2} - |d_0(\infty)|^2 = \frac{1}{2}\left[1 - \exp\left(-2\pi\frac{h(t)}{|kvg_0|}\right)\right], \tag{42}$$

with

$$h(t) = \frac{2K^2}{\sqrt{1+|\alpha|^2}} = \frac{\dot{\alpha}^2(t)}{(\sqrt{1+|\alpha|^2})^{5/2}}. \tag{43}$$

This constitutes the main result of our paper. We note the dark state probability after crossing a node becomes

$$P = 1 - |C_+(\infty)|^2 - |C_-(\infty)|^2 = \exp\left(-2\pi\frac{h(t)}{|kvg_0|}\right). \tag{44}$$

To our knowledge, this result has not been derived before. As we will show in the following through extensive comparisons with detailed numerical simulations, this result completely captures the physics of population transfer due to nonadiabatic level crossing induced by the center of mass motion of the Lambda-type 3-level atom coupled to two laser fields. It leads to the conclusion that the larger the atomic speed v_z is, the more reasonable it is to adopt the approximation of taking $\alpha(t)$ and $K(t)$ as constants and neglect the term $2iK^2\int_{-u}^{t}\exp[2i\int_{t'}^{t}\varepsilon(t'')dt''/\hbar]\varepsilon(t')C_+(t')dt'/\hbar$. Furthermore as we shall see in the next section, even in the limit of a small v_z, the transition probability (44) as given by the analytic Landau-Zener method also compares well with results from numerical simulations.

B. Three-dimensional motion of atoms

In the limit as considered presently when atomic motion is predetermined, a full three dimensional center of mass motion of the atom can be discussed without much further complications. Essentially, it is the component of the atomic

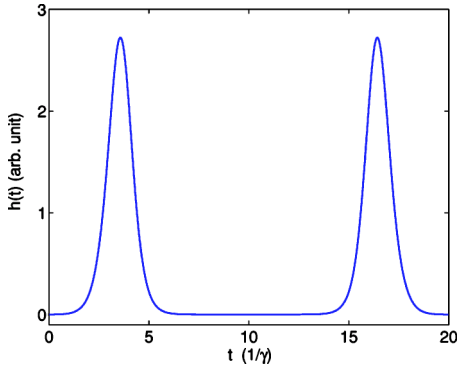

FIG. 5. The function $h(t)$.

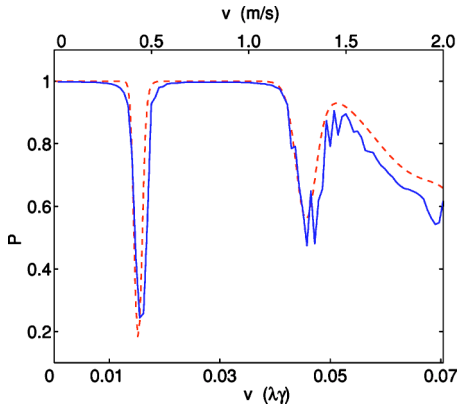

FIG. 6. The dark state survival probability P after crossing a nodal plane when the atomic motion corresponds to a constant speed along the cavity axis. The solid line comes from the numerical simulation of the nodal crossing dynamics by solving Eqs. (12) for $C_j(t)$, while the dashed line is the prediction of our approximate analytic result Eq. (44) from the Landau-Zener theory.

velocity along the cavity axis direction that is involved in the level crossing dynamics, motion in the orthogonal directions only causes the crossing to be at different radial locations, thus different level spacing characteristics.

IV. RESULTS AND DISCUSSIONS

In this section, we investigate the dark state survival probability by comparing the analytic result (44) under the Landau-Zener approximation with numerical solutions of Eq. (12).

Unless otherwise noted, the parameter $g_0=(2\pi)50$ (MHz) is used, corresponds to the $\bar{g}$ at the end of Sec. II of Ref. [5]. The atomic mass for Cs is $M\approx 133\times 1.67\times 10^{-27}$ (kg).

We assume the pump shape is given by Eq. (14) where $\alpha_0=30, T_0=3\times 10^{-7}$ (s) $\sim 10\gamma$ (so that the total operation occurs within $2T_0=20/\gamma$, as typical for the optimal STIRAP process), and $t_W=T_0/3$. Therefore $t\in(0,2T_0)$.

From the approximate Landau-Zener result Eq. (44), it is easy to see that the atom's dark state survival probability P after crossing a node is closely related to the function $h(t)$ of Eq. (43). The larger is $h(t)$, the smaller is P. We show the time dependence of $h(t)$ in Fig. 5. It resembles the function $f(t)$ as shown before in Fig. 4. The duration of the state transfer protocol is taken to be $20/\gamma$ so that the (unavoidable) maximums of $h(t)$ are clearly displayed.

It is easy to see that at times near $t=3.3/\gamma$ or $t=16.7/\gamma$, $h(t)$ becomes rather large. If an atom crosses a node at these instants, the transition probability to other states may become significant. This corresponds to the qualitative picture of the adiabatic breakdown as mentioned in the preceding section.

As a simple example, we assume the atom moves with a constant speed v. At time $t=0$ when the state transfer protocol begins, the atom is at the peak of the cavity field where $|\sin(kz)|=1$. In Fig. 6 we present the results for the dark state survival probability P (as a function of v) at $t=20/\gamma$, after the internal state transfer protocol has been completed.

The two prominent features of small P valleys can be easily understood. They correspond, respectively, to the crossing of a nodal plane at instants when $h(t)$ is large as in Fig. 5, by slow and fast moving atoms. If the atomic speed is small enough, e.g., when $v<0.01(\lambda\gamma)=0.28$ (m/s), P remains essentially unity. This is because with this speed, the atom cannot arrive at the nearest node before the state transfer protocol is completed. When v is increased to $0.017(\lambda\gamma)=0.47$ (m/s), the first small P valley shows up, corresponding to the atom arriving at the nodal plane at about $t=16.7/\gamma$ when $h(t)$ is significant (near its second peak). The second small P valley corresponds to the atomic speed of $0.049(\lambda\gamma)=1.36$ (m/s), when the atom arrives at the nodal plane at about $t=3.3/\gamma$ when $h(t)$ is around its first temporal peak. As we have analyzed in the preceding section, this second peak corresponds to the beginning of the state transfer protocol. If the atom leaves the dark state at this time, the whole operation will be destroyed.

We also note that the minimum of P near the second small P valley when $v\sim 0.049(\lambda\gamma)=1.36$ (m/s) is larger than the minimum of the first small P valley of $v\sim 0.017(\lambda\gamma)=0.4$ (m/s). This can be easily explained according to the analytic result Eq. (44), $P=\exp[-2\pi h(t)/|kvg_0|]$, which shows that for the same value of $h(t)$, P is larger for larger v. When the atomic speed is larger than $v\sim 0.049(\lambda\gamma)=1.36$ (m/s), the atom will cross more than one node during the operation time, and the dark state survival probability becomes even smaller. We can approximate in this case $P\approx\Pi_{i=1}^{n}P_i$ where n is the number of nodes crossed by the atom and P_i is the probability for the atom to remain in the dark state after crossing the ith node. This constitutes an excellent approximation when n is small.

In practice, the atom may be trapped in an additional potential, e.g., takes a harmonic motion instead of a straight line. In the optimal scenario when the center of the harmonic trap overlaps the peak of the cavity field standing wave, and when the operation starts at the instant when the atom is located at the trap center, the corresponding results for this case is presented in Fig. 7, where we have further assumed a typical trap frequency $\omega_T\sim 1.32$ (MHz). We note that the atom's final dark state survival probability is related to its initial speed v as well.

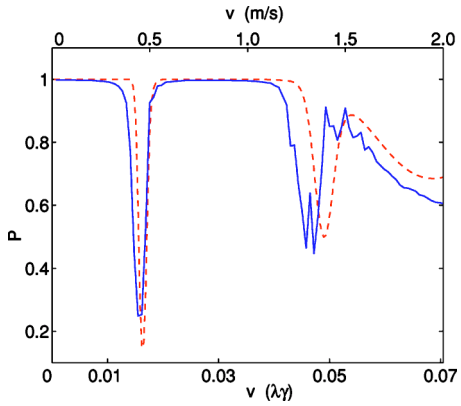

FIG. 7. The same as in Fig. 6 but for a predetermined oscillation of the atom as confined in an external harmonic trap. This external trap can be a magnetic trap or an optical dipole trap from additional lights not involved in forming the dark state.

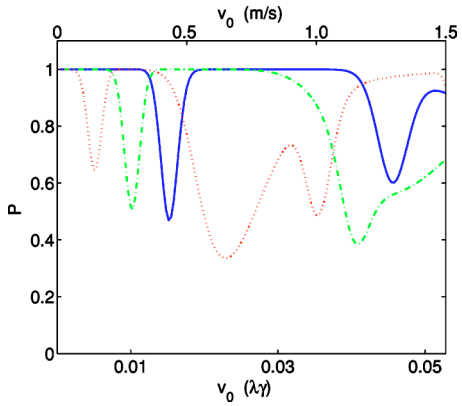

FIG. 8. P as a function of v_0 for the initial atomic locations along cavity axis $z_0=\lambda/4,\lambda/3$, and $5\lambda/12$.

This figure resembles that of Fig. 6, with the main difference being the minimum of P in the two valleys being smaller here. This is because in an harmonic motion, its speed at the nodal plane is smaller than its initial speed v.

It is remarkable that despite of the approximations used in deriving the analytic Landau-Zener transition rate Eq. (44), it gives rise to results that show an overall agreement with the fully numerical simulations of Eq. (12). This demonstrates convincingly that at least in the parameter regime being considered by us, our result Eq. (44) captures the complete physics involved in this model problem.

A. The velocity dependence

To gain some understanding of the effects due to the unavoidable momentum distribution of the atom, we assume here a one-dimensional distribution (for the speed of the atomic center of mass)

$$f(v)=\frac{1}{A}\exp\left[-\frac{(v-v_0)^2}{(\Delta v)^2}\right], \tag{45}$$

centered at a central velocity v_0 and with a distribution width $\Delta v=1.2\times10^{-3}(\lambda\gamma)$ [0.035 (m/s)], or about 10 times Cs recoil velocity. The normalization constant is given by

$$A(v_0,\Delta v)=\int_0^\infty \exp\left[-\frac{(v-v_0)^2}{(\Delta v)^2}\right]dv. \tag{46}$$

In the following, we consider $v_0\in[0,5.3]\times10^{-2}(\lambda\gamma)$, i.e., [0,1.5] (m/s). We note that for each v_0, the above distribution (45) is essentially bounded from above by $v_{\max}\sim v_0+2\Delta v$. When $v_0=5.3\times10^{-2}(\lambda\gamma)=1.44$ (m/s), we find $v_{\max}\sim5.5\times10^{-2}(\lambda\gamma)=1.5$ (m/s) and $v_{\max}2T_0/(\lambda/2)=2.21$, i.e., for $v_0\leqslant5.3\times10^{-2}(\lambda\gamma)$, the atom will cross at most three nodes.

The dark state survival probability as a function of v_0 can then be approximately computed according to

$$P(v_0)=\frac{B(v_0)}{A(v_0)}, \tag{47}$$

where

$$\begin{aligned}B(v_0)\approx&\int_0^{\lambda/(4\times2T_0)}\exp\left[-\frac{(v-v_0)^2}{(\Delta v)^2}\right]dv\\&+\int_{\lambda/(4\times2T_0)}^{3\lambda/(4\times2T_0)}\exp\left[-\frac{(v-v_0)^2}{(\Delta v)^2}\right]P_1(v)dv\\&+\int_{3\lambda/(4\times2T_0)}^{5\lambda/(4\times2T_0)}\exp\left[-\frac{(v-v_0)^2}{(\Delta v)^2}\right]P_1(v)P_2(v)dv\\&+\int_{5\lambda/(4\times2T_0)}^{7\lambda/(4\times2T_0)}\exp\left[-\frac{(v-v_0)^2}{(\Delta v)^2}\right]P_1(v)P_2(v)P_3(v)dv,\end{aligned}$$

and $P_1(v),P_2(v)$, and $P_3(v)$ are, respectively, the dark state survival probability after crossing the first, the second, and the third node. In the above discussion, we have assumed that the atomic initial position is $z_0=\lambda/4$, where the cavity field has its maximal value. The $P(v_0)$ for other values of $z_0\neq0$ can be obtained similarly.

In Fig. 8, we have presented the numerically computed dark state survival probability P as a function of v_0 for several different atomic initial positions z_0.

B. Three-dimensional atomic motion

To complete this study, we present selective results for the three-dimensional atomic motion in this section. We selected two different situations where the atom is initially at the antinodal point of the cavity field mode, and is taking a straight line motion that makes an angle of 30° or 60° with respect to the cavity axis. (See Figs. 9 and 10.) Not surprisingly, we again find excellent agreement with our analytic Landau-Zener result Eq. (44), applied appropriately as discussed earlier with the velocity component along the cavity axis being used to parametrize level crossing, essentially the same as the case of the one-dimensional model considered earlier.

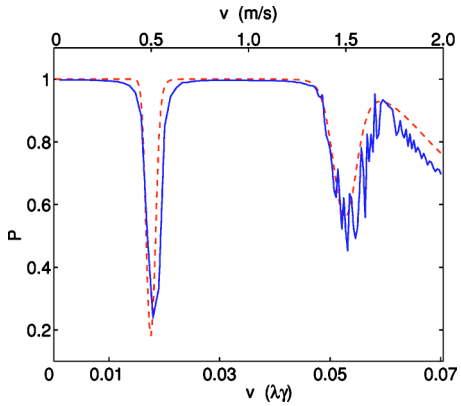

FIG. 9. The dark state survival probability P after crossing a nodal plane when the atomic motion corresponds to a constant speed along the direction 30° off the cavity axis. The solid line comes from the numerical simulation of the nodal crossing dynamics by solving the Eqs. (12) for $C_j(t)$, while the dashed line is the prediction of our approximate analytic result Eq. (44) from the Landau-Zener theory.

C. The complete analytic solution for the resonant case

The various results illustrated above clearly show that our approximate Landau-Zener solution Eq. (44) captures the essential physics for the level crossing dynamics of the atom cavity model described by Eqs. (12). It turns out that the complete analytic solution to Eqs. (12) is available from the earlier work of Ref. [14]. Through a mapping of our model, we find that the exact result is given by

$$P = (1 - \mathcal{P} - \mathcal{Q})^2 \tag{48}$$

with

$$\mathcal{P} = \exp(-2\pi|p|),$$

$$\mathcal{Q} = \exp(-2\pi|q|), \tag{49}$$

and $p = q = |K|^2/[2kvg_0\sqrt{1+|\alpha(t)|^2}]$. More explicitly, the exact result can be casted in the form

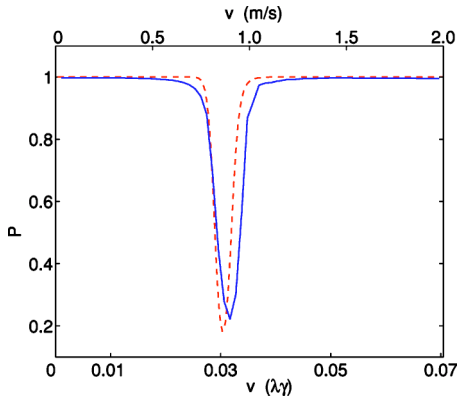

FIG. 10. The same as in Fig. 9 but for atomic motion 60° off the cavity axis. Only one small P valley shows up within the velocity range because of the large angle off the cavity axis.

$$P = \left\{1 - 2\exp\left[-\pi\frac{\dot{\alpha}^2}{2kg_0|v|(1+|\alpha|^2)^{5/2}}\right]\right\}^2$$

$$= \left[1 - 2\exp\left(-\pi\frac{h(t)}{2|kvg_0|}\right)\right]^2. \tag{50}$$

Expressed in terms of a series expansion of the above exponent, the exact result (50) is the same as the approximate one (44) up to the first order. For all the parameters considered in this work, the two are essentially indistinguishable because the exponent is relatively small as confirmed by our numerical simulations. For very small v (or not so small an exponent), however, the two differs, because the rapid oscillating term neglected (see Appendix C) is not necessary small anymore.

V. SUMMARY

In conclusion, we have studied nonadiabatic motional effects of a three-level Λ-type atom Raman coupled to the standing wave quantum field of a high-Q optical cavity and an external pump field sharing the same spatial profile.

First, making use of the Landau-Zener approximation to the crossing of a nodal plane by the atom, we have derived an analytic formula describing the survival probability for the atom to stay in the so-called motional insensitive dark state. Surprisingly, our numerical results show that the approximation is remarkably good within current experimental parameters, thus can be used to guide the experimental implementation of the motional insensitive protocol [5].

Second, we find that the nonadiabatic motional effects is essentially connected with the dimensionless parameter $v \times (20/\gamma)$, the distance the atom (with center of mass velocity v) travels during the state transfer protocol of $\sim 20/\gamma$. If this distance becomes a significant fraction of λ, i.e., $v \times (20/\gamma) \geqslant \lambda/4$, or $v \geqslant \lambda\gamma/(48) = 0.577$ (m/s), then nonadiabatic effect will spoil the motional insensitive protocol in general, even if the atom is assumed to be located initially near the antinodal planes of $\sin(kz) = \pm 1$.

To be sure of the adiabatic following of the dark state, one needs to assure at all times

$$(2\pi)\frac{h(t)}{|kvg_0|} \ll 1, \tag{51}$$

and the number of nodes crossed is small.

Finally, we hope to clarify whether the transition probability is insensitive or sensitive to the motional effects for the model problem studied. If the atom oscillates in a trap but does not cross the node, as in the case considered in Ref. [5] and attempted in the recent Caltech experiment [1] (where the coupling typically varies by a factor of 2), the result is relatively insensitive to the motional effects. On the other hand, if the atom moves across the node (e.g., if there is no additional trapping due to FORT beams), the transition probability is more sensitive to the motional effects. When the light field from a different longitudinal mode of the cavity is used to trap the atom [1], there is no guarantee that the atom will avoid the nodal crossing points even if it is relatively localized around a trap field node/antinode, because the cav-

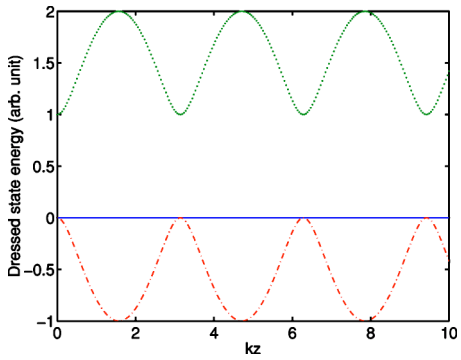

FIG. 11. Similar to Fig. 2 but for $\Delta \neq 0$.

ity and trap field standing waves are of different periods.

ACKNOWLEDGMENTS

The authors thank Dr. Y. X. Miao for helpful communications. The authors acknowledge the support of CNSF, the Knowledged Innovation Program (KIP) of the Chinese Academy of Science, and the National Fundamental Research Program of China (No. 001CB309310). L. Y. also acknowledges the support of NSF.

APPENDIX A: THE CASE OF A NONZERO DETUNING ($\Delta \neq 0$)

When $\Delta \neq 0$, the Hamiltonian in the interaction picture with the same basis $|\{|e,0\rangle,|s,1\rangle,|g,0\rangle\}$ becomes

$$H = \begin{pmatrix} \Delta & g & \Omega \\ g^* & 0 & 0 \\ \Omega^* & 0 & 0 \end{pmatrix}. \tag{A1}$$

The three eigenvalues are

$$E_0 = 0,$$

$$E_\pm = \tfrac{1}{2}\Delta \pm \sqrt{4g^2 + 4\Omega^2 + \Delta^2}, \tag{A2}$$

with the corresponding eigenstates $|D\rangle$ and $|E_\pm\rangle$. Clearly at nodal planes when $\sin(kz)=0, |E_\pm|$ take their minimal values

$$|E_+|_{\max} = \Delta,$$

$$|E_-|_{\min} = 0, \tag{A3}$$

as shown in Fig. 11, on inspecting of which leads to the following two comments.

First, irrespective of whether $\Delta=0$ or $\Delta\neq 0$, the dressed state energy levels cross at the nodal planes $\sin(kz)=0$.

Second, when $\Delta=0$, all three energy levels have the same value zero at the nodal planes, while for $\Delta\neq 0$, only E_- and E_0 take zero values. There is a gap for E_+ whose width is Δ. Thus if Δ is large enough, the transition from dark state $|D\rangle$ to $|E_+\rangle$ can be avoided, but to state $|E_-\rangle$ remains because of the degeneracy at the crossing. The total transition probability again can be calculated theoretically using the previously adopted Landau-Zener approximation.

To compute the transition probability for $\Delta\neq 0$, we expand the state of the atom plus the field in terms of the eigenbasis Eqs. (3) and (8) of the system Hamiltonian for $\Delta=0$, which is now

$$|D\rangle = \frac{1}{\sqrt{1+|\alpha(t)|^2}}(|g_1,0\rangle - \alpha(t)|g_0,1\rangle),$$

$$|B_\pm\rangle = \frac{1}{\sqrt{2}}(|B\rangle \pm |e,0\rangle), \tag{A4}$$

with the corresponding eigenvalues Eq. (7) re-expressed in this appendix as

$$\epsilon_0 = 0,$$

$$\epsilon_\pm = \pm\chi[r(t)]|g_0|\sqrt{1+|\alpha(t)|^2}. \tag{A5}$$

As before in Eq. (8), we have introduced

$$|B\rangle = \frac{1}{\sqrt{1+|\alpha(t)|^2}}[|g_1,1\rangle + \alpha(t)|g_0,0\rangle],$$

and the parameter r_0 has been assumed to be unity. Then the system Hamiltonian including Δ is

$$H = \Delta|e,0\rangle\langle e,0| + \epsilon_+|B_+\rangle\langle B_+| + \epsilon_-|B_-\rangle\langle B_-|.$$

Noting that

$$|e,0\rangle = \frac{1}{\sqrt{2}}(|B_+\rangle - |B_-\rangle),$$

we rewrite Eq. (A1) as

$$H = \left(\epsilon_+ + \frac{\Delta}{2}\right)|B_+\rangle\langle B_+| + \left(\epsilon_- + \frac{\Delta}{2}\right)|B_-\rangle\langle B_-| - \frac{\Delta}{2}(|B_+\rangle\langle B_-| + |B_-\rangle\langle B_+|). \tag{A6}$$

Expanding the quantum state as in Eq. (9),

$$|\Psi(t)\rangle = C_0|D\rangle + C_+e^{-i\int_0^t[\epsilon_+(t')+\Delta]dt'}|B_+\rangle + C_-e^{-i\int_0^t[\epsilon_-(t')+\Delta]dt'}|B_-\rangle, \tag{A7}$$

we obtain the following equations:

$$\dot{C}_0 = -(C_+e^{-i\int_0^t[\epsilon(t')+\Delta]dt'} + C_-e^{-i\int_0^t[-\epsilon(t')+\Delta]dt'})K,$$

$$\dot{C}_+ = C_0e^{i\int_0^t[\epsilon(t')+\Delta]dt'}K + i\frac{\Delta}{2}(C_-e^{i\int_0^t 2\epsilon(t')dt'} + C_+),$$

$$\dot{C}_- = C_0e^{i\int_0^t[-\epsilon(t')+\Delta]dt'}K + i\frac{\Delta}{2}(C_+e^{-i\int_0^t 2\epsilon(t')dt'} + C_-). \tag{A8}$$

Since

$$\dot{C}_\pm = e^{\pm i\int_0^t 2\epsilon(t')dt'}\dot{C}_\mp, \tag{A9}$$

we can integrate it to obtain

$$C_{\pm} = \int \dot{C}_{\mp}(t') e^{\pm i \int_0^{t'} 2\epsilon(t'')dt''} dt' \simeq C_{\mp} e^{\pm i \int_0^t 2\epsilon(t')dt'}, \tag{A10}$$

where we have neglected the "small term" $\int C_{\mp}(t')d \exp[\pm i \int_0^{t'} 2\epsilon(t'')dt'']$ (as in Sec. III and Appendix C). Then according to Eq. (A8), we have

$$\dot{C}_+ = C_0 e^{i \int_0^t [\epsilon(t')+\Delta]dt'} K + i\Delta C_+,$$

$$\dot{C}_- = C_0 e^{i \int_0^t [-\epsilon(t')+\Delta]dt'} K + i\Delta C_-. \tag{A11}$$

Assuming $C_{\pm} = e^{i\Delta t}\xi_{\pm}$, the above equation can be expressed as

$$\dot{\xi}_{\pm} = C_0 e^{\pm i \int_0^t \epsilon(t')dt'} K, \tag{A12}$$

which when coupled with the equation

$$\begin{aligned} \dot{C}_0 &= -(C_+ e^{-i \int_0^t [\epsilon(t')+\Delta]dt'} + C_- e^{-i \int_0^t [-\epsilon(t')+\Delta]dt'})K \\ &= -(\xi_+ e^{-i \int_0^t \epsilon(t')dt'} + \xi_- e^{-i \int_0^t \epsilon(t')dt'})K, \end{aligned} \tag{A13}$$

is formally the same as equations for $\Delta = 0$. Thus we obtain the same result

$$|C_0|^2 = 1 - |\xi_+|^2 - |\xi_-|^2 = \exp\left[-2\pi \frac{h(t)}{|kvg_0|}\right]. \tag{A14}$$

To obtain Eq. (A14) we need to neglect the rapidly oscillating term $\int \xi_{\mp}(t')d \exp[\pm i \int_0^{t'} 2\epsilon(t'')dt'']$. When Δ is large compared to $\sqrt{|V|}[V = kvg_0\sqrt{1+|\alpha(t)|^2}]$, the two terms $\int \xi_{\mp}(t')d \exp[\pm i \int_0^{t'} 2\epsilon(t'')dt'']$, $\int C_{\mp}(t')d \exp[\pm i \int_0^{t'} 2\epsilon(t'')dt'']$ cannot be neglected simultaneously. If $C_{\mp}$ is a slowly varying function of time t, $\xi_{\mp}$ will be a fast varying one thus it cannot be considered as a constant in the integration. Therefore, the result (A14) is applicable only when Δ is not much larger than $\sqrt{|V|}$.

When the effect of Δ is not negligible, we can estimate its influence by performing a simple perturbation calculation. Expressing Eq. (A8) in a matrix form,

$$i\frac{d}{dt}\vec{C} = \mathcal{M}(t)\vec{C}. \tag{A15}$$

with $\vec{C} = (C_+, C_0, C_-)^T$ and the time dependent coefficient matrix $\mathcal{M}$.

The evolution operator S defined as $\vec{C}(+\infty) = S\vec{C}(-\infty)$ can be expanded as a series of $\mathcal{M}$,

$$S = 1 - i\int_{-\infty}^{\infty} \mathcal{M}(t)dt - \int_{-\infty}^{\infty}\int_{-\infty}^{t} \mathcal{M}(t)\mathcal{M}(t')dt\,dt' + \cdots. \tag{A16}$$

With this formula and the initial condition $\vec{C}(-\infty) = (0,1,0)^T$, we obtain the dark state probability after crossing a mode up to the first order in Δ,

$$P = 1 - \frac{\pi|K|^2}{|V|}\left(4 + \Delta\sqrt{\frac{2\pi}{|V|}}\right). \tag{A17}$$

We note that the zeroth order term $1 - 4\pi|K|^2/|V|$ is exactly the same as that for the resonant case (within the first order perturbation theory).

APPENDIX B: THE LINEAR APPROXIMATION

Within the discussion as in Sec. II B, we mapped our level crossing problem into the well-known problem of Landau-Zener transition.

As was shown before, the adiabatic condition is

$$\left|\frac{f(t)}{\sin(kz)}\right| \ll 1, \tag{B1}$$

with the typical behavior for $f(t)$ as shown in Fig. 4. Taking $f(t) \leqslant 0.035$, we see that within the domain of $|\sin(kz)| < 0.7$, we have

$$\min\left|\frac{f(t)}{\sin(kz)}\right| < 0.05, \tag{B2}$$

although still much less than 1. Thus we can define the domain $|\sin(kz)| < 0.7$ as the domain of validity where the adiabatic condition is marginal. In this domain, the error of the linear approximation $\sin(kz) \sim kz$ is about 10%.

APPENDIX C: THE SMALL TERM

In this appendix, we provide the justification for the neglect of the second term of Eq. (34).

Given that initially the atom is in the dark state, we need $C_+(t')$ to be small in order to maintain adiabatic operation. Thus, we approximate

$$C_- = e^{-2i\int_0^{t'} \varepsilon(t'')dt''/\hbar} C_+ + 2i\int_{-u}^{t} e^{-2i\int_0^{t'} \varepsilon(t'')dt''/\hbar} \varepsilon(t') C_+(t')dt'/\hbar, \tag{C1}$$

where u is the end of the time domain and assumed to satisfy $|\sin(kvu)| = 0.7$.

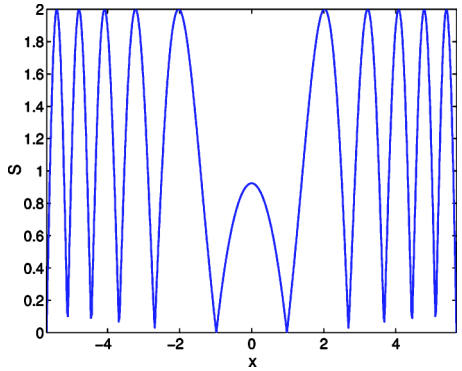

FIG. 12. The term $S(x)$ as a function of x for $v = 3.5 \times 10^{-2}(\lambda\gamma)$.

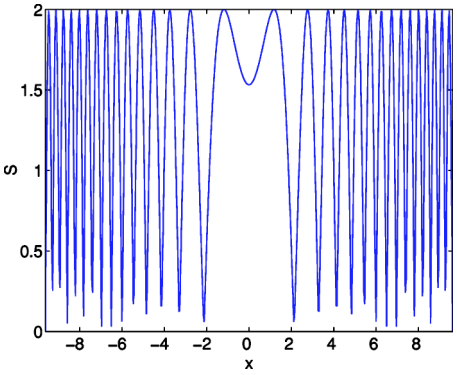

FIG. 13. The same as in Fig. 12 but for $v=1.2\times10^{-2}(\lambda\gamma)$.

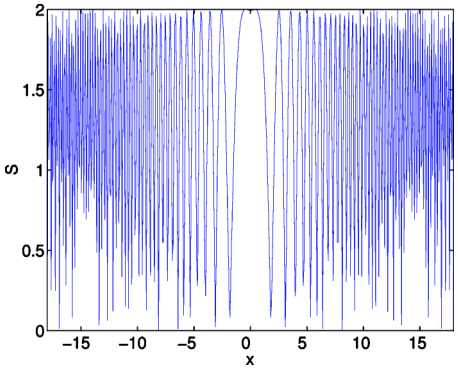

FIG. 14. The same as in Fig. 12 but for $v=3.5\times10^{-3}(\lambda\gamma)$.

We first approximate the second term of Eq. (C1) according to

$$\left|2i\int_{-u}^{t}e^{-2i\int_0^{t'}\varepsilon(t'')dt''/\hbar}\varepsilon(t')C_+(t')dt'/\hbar\right| \sim \left|2i\int_{-u}^{t}e^{-2i\int_0^{t'}\varepsilon(t'')dt''/\hbar}\varepsilon(t')dt'C_+(t)/\hbar\right|. \quad \text{(C2)}$$

We note that

$$\begin{aligned} S &= \left|2i\int_{-u}^{t}e^{-2i\int_0^{t'}\varepsilon(t'')dt''/\hbar}\varepsilon(t')dt'/\hbar\right| \\ &= 2\left|\int_{-u}^{t}e^{-2i\int_0^{t'}kvt''g_0\sqrt{1+|\alpha|^2}dt''}kvt'g_0\sqrt{1+|\alpha|^2}\,dt'\right| \\ &\approx 2\left|\int_{-u}^{t}e^{-ikvt'^2g_0\sqrt{1+|\alpha|^2}}kvt'g_0\sqrt{1+|\alpha|^2}\,dt'\right| \\ &= 2\left|\int_{-\Omega u}^{\Omega t}e^{-i\tau'^2}\tau'\,d\tau'\right|, \end{aligned} \quad \text{(C3)}$$

where we have approximated $\alpha(t)$ as a constant and denoted

$$\Omega=\sqrt{kvg_0\sqrt{1+|\alpha|^2}},$$

$$\tau'=\Omega t'. \quad \text{(C4)}$$

Thus

$$S=2\left|\int_{-\Omega u}^{\Omega t}e^{-i\tau'^2}\tau'\,d\tau'\right| \quad \text{(C5)}$$

$$=2\left|\int_{-\sqrt{kvg_0\sqrt{1+|\alpha|^2}}(0.77/kv)}^{\sqrt{kvg_0\sqrt{1+|\alpha|^2}}t}e^{-i\tau'^2}\tau'\,d\tau'\right|, \quad \text{(C6)}$$

where we have used $\sin^{-1}0.7=0.77$.

We take the worst case and use the value of α when $\dot{\alpha}$ is maximum. This leads to

$$\alpha=30\times\exp\left[-\frac{(1\times10^{-7}-6\times0.5\times10^{-7})^2}{10^{-14}}\right]\approx0.55,$$

$$\sqrt{1+|\alpha|^2}=1.14, \quad \text{(C7)}$$

and $\sqrt{kvg_0\sqrt{1+|\alpha|^2}}=5.0\times10^7\sqrt{v}$. If we now take $t=s/(kv)$, we find

$$S=2\left|\int_{-\sqrt{kvg_0\sqrt{1+|\alpha|^2}}(0.77/kv)}^{\sqrt{kvg_0\sqrt{1+|\alpha|^2}}(s/kv)}e^{-i\tau'^2}\tau'\,d\tau'\right| \quad \text{(C8)}$$

$$=2\left|\int_{-5.69/\sqrt{v}}^{x}e^{-i\tau'^2}\tau'\,d\tau'\right|, \quad \text{(C9)}$$

with

$$x=\sqrt{kvg_0\sqrt{1+|\alpha|^2}}\frac{s}{kv}. \quad \text{(C10)}$$

The oscillating behaviors of S for $v=3.5\times10^{-2}(\lambda\gamma)$ [1(m/s)], $1.2\times10^{-2}(\lambda\gamma)$ [0.35(m/s)], and $v=3.5\times10^{-3}(\lambda\gamma)$ [0.1(m/s)] are shown below in Figs. 12–14.

We see that the amplitude of S is about 2, not really a small value. On the other hand, S is a rapid oscillation function of time t, thus does not lead to much effect during the dynamic evolution. We believe this is the reason why our Landau-Zener result based on the neglect of this "small term" is justified by the numerical simulations.

[1] J. McKeever, J. R. Buck, A. D. Boozer, A. Kuzmich, H.-C. Naegerl, D. M. Stamper-Kurn, and H. J. Kimble, Phys. Rev. Lett. **90**, 133602 (2003).
[2] C. J. Hood *et al.*, Science **287**, 1447 (2000).
[3] J. A. Sauer, K. M. Fortier, M. S. Chang, C. D. Hamley, and M. S. Chapman, quantph/0309052 (unpublished); A. B. Mundt, A. Kreuter, C. Becher, D. Leibfried, J. Eschner, F. Schmidt-Kaler, and R. Blatt, Phys. Rev. Lett. **89**, 103001 (2002); T. Fischer, P. Maunz, P. W. H. Pinkse, T. Puppe, and G. Rempe, *ibid.* **88**, 163002 (2002).

[4] T. A. B. Kennedy and P. Zhou, Phys. Rev. A **64**, 063805 (2001).
[5] L.-M. Duan, A. Kuzmich, and H. J. Kimble, Phys. Rev. A **67**, 032305 (2003).
[6] A. S. Parkins, P. Marte, P. Zoller, and H. J. Kimble, Phys. Rev. Lett. **71**, 3095 (1993).
[7] C. K. Law and J. Kimble, J. Mod. Opt. **44**, 2067 (1997); J. Eberly and C. K. Law, Acta Phys. Pol. A **93**, 55 (1998).
[8] A. Kuhn *et al.*, Appl. Phys. B: Lasers Opt. **69**, 373 (1999); H. Nha *et al.*, Phys. Rev. A **63**, 010301 (2001).
[9] J. Ye, D. W. Vernooy, and H. J. Kimble, Phys. Rev. Lett. **83**, 4987 (1999).
[10] L. D. Landau, Phys. Z. Sowjetunion **2**, 46 (1932); C. Zener, Proc. R. Soc. London, Ser. A **137**, 696 (1932).
[11] A. C. Doherty, A. S. Parkins, S. M. Tan, and D. F. Walls, J. Opt. B: Quantum Semiclassical Opt. **1**, 475 (1999).
[12] L. You, Phys. Rev. A **64**, 012302 (2001).
[13] C. P. Sun, Phys. Rev. D **41**, 1318 (1990).
[14] C. E. Carroll and F. T. Hioe, J. Phys. A **19**, 2061 (1986).